

# Substitution of samarium for strontium in the structure of hydroxyapatite

*E.I.Getman, A.V.Ignatov, S.N.Loboda,  
Mohammed A.B.Abdul Jabar, A.O.Zhegailo, A.S.Gluhova*

Donetsk National University, 24 Universitetskaya Str.,  
83001 Donetsk, Ukraine

*Received April 6, 2011*

Substitution of samarium for strontium in hydroxyapatite corresponded to the scheme  $\text{Sr}^{2+} + \text{OH}^- \rightarrow \text{Sm}^{3+} + \text{O}^{2-}$  has been investigated by X-ray powder diffraction and IR spectroscopy. It was established that solid solutions  $\text{Sr}_{10-x}\text{Sm}_x(\text{PO}_4)_6(\text{OH})_{2-x}\text{O}_x$  are formed in the range of  $x = 0-1.6$  at  $1100^\circ\text{C}$  in air. Crystal features of some samples have been refined by Rietveld method. It was shown that  $\text{Sm}^{3+}$  preferably occupy the Sr(2) site. The hydroxyapatite dehydration occurring under the scheme  $2\text{OH}^- \rightarrow \text{O}^{2-} + \square$  was confirmed by IR spectra of obtained samples.

Методом рентгенофазового анализа и ИК-спектроскопии изучено изоморфное замещение стронция на самарий в гидроксиапатите в соответствии со схемой замещения  $\text{Sr}^{2+} + \text{OH}^- \rightarrow \text{Sm}^{3+} + \text{O}^{2-}$ . Установлено, что однофазные твердые растворы состава  $\text{Sr}_{10-x}\text{Sm}_x(\text{PO}_4)_6(\text{OH})_{2-x}\text{O}_x$ , синтезированные при температуре  $1100^\circ\text{C}$ , образуются в области составов  $x = 0-1.6$ . Кристаллическая структура некоторых образцов уточнялась с помощью алгоритма Ритвельда. Установлено, что ионы  $\text{Sm}^{3+}$  преимущественно заселяют позицию Sr(2) структуры апатита. Методом ИК-спектроскопии установлено протекание дегидратации гидроксиапатита в полученных образцах по схеме  $2\text{OH}^- \rightarrow \text{O}^{2-} + \square$ .

## 1. Introduction

The interest of researchers to compounds with the structure of apatite is caused by an opportunity of their practical application. So they are used as artificial biomaterials compatible with a bone tissue, luminophor materials, sensor controls of moisture and alcohols, adsorbents of ecologically harmful and radioactive substances, catalysts of alcohols dehydration reactions and hydrolysis of chlorbenzene, conversion of methane and other cases [1-6]. In addition, it should be noted that there exists a possibility of structure units replacement by others in the compounds with the structure of apatite. The solid solutions formed in this way can essentially enlarge the wide area of their practical application inasmuch as the incorporation of modifying ions into the structure of apatite can results in an appearance

of new useful physicochemical properties. Therefore, it is not surprising that a great number of research works devoted to the investigation of substitutions in the structure of apatite has been reported in the literature in recent years. However, the substitutions in calcium hydroxyapatite were mainly investigated, while the substitutions in strontium hydroxyapatite virtually have not been examined. Therefore, the purpose of this study is to investigate the substitution of samarium for strontium in the structure of hydroxyapatite. As the charge of substituent  $\text{Sm}^{3+}$  differs from the charge of substituted  $\text{Sr}^{2+}$ , the simultaneous replacement of  $\text{OH}^-$  groups by  $\text{O}^{2-}$  ions would take place to keep the charge balance in the modified apatite. In this connection, the substitution of samarium for strontium can be described by the following scheme:

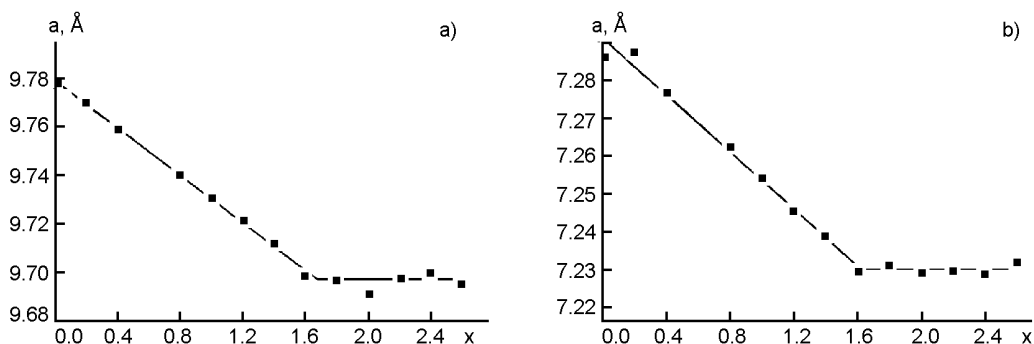
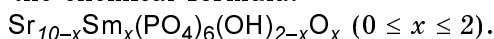


Fig. 1. Dependence of the unit cell dimensions of strontium hydroxyapatite modified by samarium versus composition.

$\text{Sr}^{2+} + \text{OH}^- \rightarrow \text{Sm}^{3+} + \text{O}^{2-}$ . Based on this scheme the probable composition of the formed solid solutions would be expressible by the chemical formula:



## 2. Experimental

The samples were prepared from mixtures of strontium nitrate, samarium oxide and dibasic ammonium phosphate, which were composed according to the  $(10-x)\text{Sr}(\text{NO}_3)_2 + (x/2)\text{Sm}_2\text{O}_3 + 6(\text{NH}_4)_2\text{HPO}_4$  stoichiometry for  $x$  ranging from 0 to 2.6 by step of 0.2. The mixtures were homogenized in an agate mortar for 20 min, placed in an alumina crucible and calcined at 300 and 800 °C for 3 h at each temperature. The resulting cakes were ground and homogenized for 10 min, pelletized and heated in an electric furnace at 1100°C for 5–6 h. After sintering the samples were quenched in air, powdered, and analyzed by X-ray powder diffraction. Then the samples were pelletized and sintered again. This step was repeated several times until a constant phase composition has been obtained. Total time of sintering at 1100°C came to 22 h.

X-ray powder diffraction patterns of the samples were recorded at room temperature, using a powder diffractometer DRON-2 with the Ni-filtered copper  $K_\alpha$  radiation. The scanning rate was 1°/min, Si used as an external standard. The  $a$  and  $c$  parameters of the hexagonal unit cell of hydroxyapatite were calculated from the positions of 18 most intense and sharp reflections by using a least-squares refinement program.

X-ray powder diffraction data for crystal structure refinement were collected in a step regime: step 0.05° ( $2\theta$ ), interval  $15.00 \leq 2\theta \leq 140.00$ , scanning rate 10 s per step. The profile analysis of the data was performed using the method of approxima-

tion of X-ray reflections by pseudo-Voigt profile function. The lattice parameters and crystal structure of the phases were refined using Rietveld method with the program FULLPROF.

IR spectra of the samples dispersed in KBr tablets were recorded using a Perkin-Elmer Fourier transform infrared spectrophotometer in the range 400–4000  $\text{cm}^{-1}$ .

## 3. Results and discussion

The peaks in the X-ray diffraction patterns of the samples with  $x = 0$ –1.6 are sharp and well resolved and all of them can be attributed to the hexagonal crystal form of hydroxyapatite. In the patterns of the samples with  $x = 1.8$ –2.6, apart from the peaks of hydroxyapatite, one can observe several additional reflections. We could not match those with a phase because only some few minor peaks may be visible which is not enough for the correct identification. The lattice parameters of the hexagonal unit cell are plotted against  $x$  in Fig. 1. It is seen that both  $a$  and  $c$  parameters decrease linearly as  $x$  increases from  $x = 0$ , obtain a minimum at  $x = 1.6$ , and then remain unchanged as  $x$  increases up to 2.6. The obtained results show that the substitution under the supposed scheme, namely:  $\text{Sr}^{2+} + \text{OH}^- \rightarrow \text{Sm}^{3+} + \text{O}^{2-}$ , take place in the range of  $x = 0$ –1.6. A decrease of the cell parameters with increase of dopant level of the modified hydroxyapatite is in agreement with the fact that the strontium ionic radius is larger than the samarium one (1.26 Å and 1.079 Å, respectively) [7].

The allocations of corresponding atoms by the crystallographic sites and their coordinates in the calcium hydroxyapatite, previously reported in [8], were used as starting data for the Rietveld refinement of the structure of the apatite phases obtained in the work. Atomic parameters of the sample

Table 1. Positional, isotropic thermal parameters ( $B_{iso}$ ) and occupations ( $G$ ) for  $Sr_{8.4}Sm_{1.6}(PO_4)_3(OH)_{0.4}O_{1.6}$  (space group  $P6_3/m$ ,  $a = 9.6936(2)$ ,  $c = 7.2245(2)$ ,  $R_B = 0.0730$ ,  $R_F = 0.0652$ ,  $R_P = 0.0615$ ,  $R_{WP} = 0.0792$ ,  $\chi_2 = 1.29$ )

Atom	Site	$x$	$y$	$z$	$B_{iso}, \text{\AA}^2$	$G$
Sr(1)	4 <i>f</i>	2/3	1/3	0.001(1)	0.90(9)	0.955(9)
Sm(1)	4 <i>f</i>	2/3	1/3	0.001(1)	0.90(9)	0.045(9)
Sr(2)	6 <i>h</i>	0.2327(4)	0.9874(5)	1/4	0.72(7)	0.792(6)
Sm(2)	6 <i>h</i>	0.2327(4)	0.9874(5)	1/4	0.72(7)	0.236(6)
P	6 <i>h</i>	0.403(1)	0.372(1)	1/4	0.5(2)	1
O(1)	6 <i>h</i>	0.331(2)	0.478(2)	1/4	1.1(5)	1
O(2)	6 <i>h</i>	0.578(2)	0.466(2)	1/4	1.3(6)	1
O(3)	12 <i>i</i>	0.351(1)	0.270(1)	0.070(2)	1.0(4)	1
O(4)	4 <i>e</i>	0	0	0.185(4)	1(1)	0.4
OH	4 <i>e</i>	0	0	0.185(4)	1(1)	0.1

Table 2. Selected bond distances ( $\text{\AA}$ )

Composition, $x$	0	0.4	0.8	1.2	1.6
P–O(1)	1.50(2)	1.50(2)	1.49(2)	1.48(2)	1.51(3)
P–O(2)	1.50(2)	1.50(2)	1.51(3)	1.47(3)	1.47(3)
P–O(3)×2	1.55(1)	1.55(1)	1.55(1)	1.56(1)	1.56(1)
<P–O>	1.53	1.53	1.53	1.52	1.53
Sr, Sm(1)–O(1)×3	2.58(1)	2.58(1)	2.57(2)	2.58(2)	2.56(2)
Sr, Sm(1)–O(2)×3	2.61(1)	2.62(1)	2.61(2)	2.62(2)	2.60(2)
Sr, Sm(1)–O(3)×3	2.88(1)	2.87(1)	2.85(1)	2.86(1)	2.85(2)
Sr, Sm(2)–O(1)	2.80(1)	2.81(2)	2.81(2)	2.79(2)	2.77(2)
Sr, Sm(2)–O(2)	2.49(2)	2.46(2)	2.49(2)	2.49(2)	2.54(3)
Sr, Sm(2)–O(3)×2	2.73(1)	2.72(1)	2.73(1)	2.70(1)	2.71(1)
Sr, Sm(2)–O(3)×2	2.47(1)	2.48(1)	2.48(1)	2.48(1)	2.48(1)
Sr, Sm(2)–O(4), OH	2.530(6)	2.499(6)	2.459(8)	2.424(7)	2.366(8)
Sr, Sm(2)–Sr, Sm(2)	4.255(5)	4.210(5)	4.138(6)	4.102(6)	4.018(6)

$Sr_{8.4}Sm_{1.6}(PO_4)_3(OH)_{0.4}O_{1.6}$  ( $x = 1.6$ ) as examples are represented in Table 1. Obtained values of atomic coordinates enable calculation of the interatomic distances; some of them are given in Table 2.

IR spectra of the strontium hydroxyapatite solid solutions are represented in Fig. 2. Unsubstituted strontium hydroxyapatite  $Sr_{10}(PO_4)_6(OH)_2$  displays typical absorptions arising from  $PO_4^{3-}$  (946- $\nu_1$ , 458- $\nu_2$ , 1034 and 1074- $\nu_3$ , 561 and 592  $cm^{-1}$ - $\nu_4$ ), absorbed water (broad peak in the range of 3200–3650  $cm^{-1}$  due to  $OH^-$  connected by hydrogen bonds, and 1630  $cm^{-1}$ ), hydroxyl group which are not included in water (3592  $cm^{-1}$ -stretching vibration and 430  $cm^{-1}$ -librational mode) [9, 10]. In the

spectra of the samples of substituted hydroxyapatite, the positions and intensities of absorptions arising from  $PO_4^{3-}$  are the same. There is only an apparent reduction of the absorption at 946  $cm^{-1}$ , which is probably caused by expansion of the absorption at 1034  $cm^{-1}$ . Increase of the  $x$  value is accompanied by decrease of the absorption bands arising from absorbed water and the absorption at 3592  $cm^{-1}$  and 540  $cm^{-1}$  reflecting vibrations of  $OH^-$  group. The absorption bands of  $OH^-$  virtually do not be detected even at  $x = 0.8$ . At the same time the absorption in the range of 510–530  $cm^{-1}$  reflecting vibration of  $Sm-O$  bond appears in the spectra of strontium hydroxyapatite modified by samarium. In the samples with higher samarium content, this band is

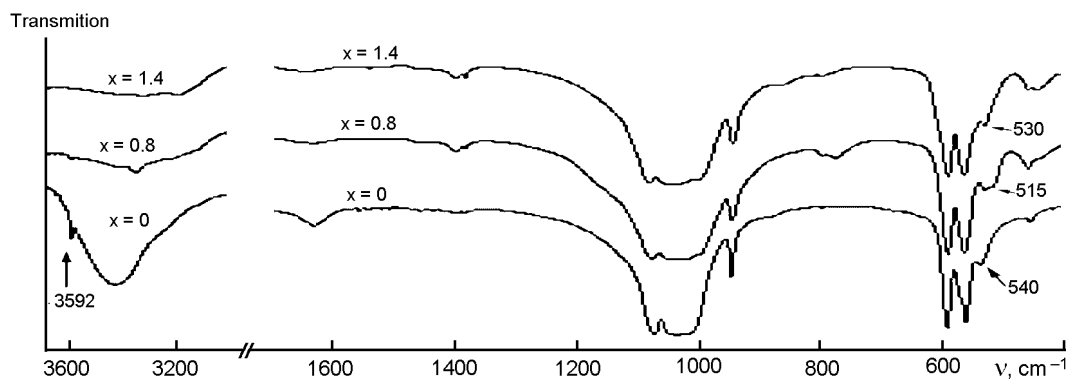


Fig. 2. IR spectra of the samples of strontium hydroxyapatite modified by samarium in the range 400–1700  $\text{cm}^{-1}$  and 3000–3700  $\text{cm}^{-1}$ .

shifted to the larger wavenumber. This fact is similar to that obtained [11, 12] from the infrared spectra of calcium hydroxyapatite modified by lanthanum and europium.

The structure of hydroxyapatite can be described on the basis of  $P6_3/m$  space group where two: Sr(1) and Sr(2) different sites for  $\text{Sr}^{2+}$  can be distinguished. The Sr(1) site is 9-fold coordinated by oxygen atoms and its size is larger than the size of Sr(2) site. The Sr(2) site is coordinated by six oxygen atoms and the  $\text{OH}^-$  group.

Previous investigations of substitutions in calcium hydroxyapatite have shown that the site preference of the substituent cation depend on its effective charge. It was established, that ion with a charge lesser than a charge of calcium mainly occupy the larger Ca(1) site whereas ion with a higher one occupy the more compact Ca(2) site [13]. This is the case for the  $\text{Sr}_{10-x}\text{Sm}_x(\text{PO}_4)_6(\text{OH})_{2-x}\text{O}_x$  system under study as well. The refinement of the crystal structure by Rietveld method has shown that  $\text{Sm}^{3+}$  having a charge higher than that of  $\text{Sr}^{2+}$  preferably occupy the Sr(2) site. In the structure of hydroxyapatite, the  $\text{OH}^-$  groups occur in columns parallel to  $c$ -axis. The main lines of the columns pass through the centres of triangles, which are formed by  $\text{Sr}^{2+}$  in the Sr(2) position. Incorporation of samarium ions into the structure of hydroxyapatite results in evident decrease of the Sm,Sr(2)–Sm,Sr(2) distance in the triangle (Table 2).

According to the scheme of substitution, the incorporation of samarium into the structure of hydroxyapatite generates the simultaneous substitution of  $\text{O}^{2-}$  for  $\text{OH}^-$  group, and  $\text{Sm}^{3+}$  on the Sr(2) site becomes the nearest neighbour of the  $\text{O}^{2-}$ . This causes a strengthening of electrostatic forces between ions arranged on the Sm,Sr(2) and OH,O(4) sites. As a result, the

total energy of the system decreases, and it promotes a process of the substitution. Bond distance of Sm,Sr(2)–OH,O(4) evidently decreases with increase of samarium content in the apatite (Table 2).

The substitution of  $\text{Sm}^{3+}$  onto the Sr(2) site should lead to decrease of the Sm,Sr(2)–O(1),(2),(3) distances since  $\text{Sr}^{2+}$  is larger than  $\text{Sm}^{3+}$ . But, as shown in Table 2, the distances remain unchanged in spite of whatever is  $x$ . Apparently this fact is the result of a balance between increasing forces of: (I) attraction of the Sm,Sr(2) cation to surrounding O(1),(2),(3),(4) anions and (II) repulsion of O(1),(2),(3) from O(4) within the coordination polyhedron.

In the IR spectra of solid solutions with  $x > 0.8$  no  $\text{OH}^-$  bands are observed, which indicate the absence of the  $\text{OH}^-$  groups in the samples. Taking into account the high temperature used for the synthesis of the samples, it is safe to say that the  $\text{OH}^-$  absence is caused by dehydration of hydroxyapatite. The similar process has been observed in the case of calcium hydroxyapatite as well [14]. So, reasoning from the fact that the base scheme of the  $\text{Sr}^{2+} + \text{OH}^- \rightarrow \text{Sm}^{3+} + \text{O}^{2-}$  substitution is accompanied by dehydration of hydroxyapatite, the formula, which describe the composition of the obtained solid solutions, requires more accurate definition. That can be formulated as  $\text{Sr}_{10-x}\text{Sm}_x(\text{PO}_4)_6(\text{OH})_{2-(x+y)}\text{O}_{x+y/2}\square_{y/2}$  (where:  $x + y \leq 2$ ) in the range of  $0 \leq x \leq 0.8$  and  $\text{Sr}_{10-x}\text{Sm}_x(\text{PO}_4)_6\text{O}_{1+x/2}\square_{1-x/2}$  in the range of  $x > 0.8$ . It should be noted that existence of  $\text{Sm}^{3+}$  substitution for  $\text{Sr}^{2+}$  in the range of  $x > 0.8$ , where no  $\text{OH}^-$  group are detected, indicates that there can also be a substitution under the scheme:  $\text{Sr}^{2+} + 1/2\square \rightarrow \text{Sm}^{3+} + 1/2\text{O}^{2-}$ . The latter scheme is a residual between the base scheme of substitu-

tion and the scheme of dehydration of hydroxyapatite. Provided that simultaneous substitution under three above-mentioned schemes really takes place but to a variable extent at different  $x$  values, definition of correct formula, which describes the composition of obtained solid solutions, is not possible at this juncture.

#### 4. Conclusion

It was established by X-ray powder diffraction that the limit for substitution of strontium for samarium in the structure of apatite is in the range of  $x = 0-1.6$ . The substitution of  $\text{Sm}^{3+}$ , which has a much smaller crystal ionic radius for  $\text{Sr}^{2+}$ , caused a decrease of unit cell parameters in the homogeneity region. The refinement by Rietveld method of crystal structure of solid solution was shown that ions  $\text{Sm}^{3+}$  preferably occupy the Sr(2) site in the structure of apatite and as a result the distance Sm,Sr(2)-Sm,Sr(2) is diminished. According to IR-spectroscopy, the formation of solid solution under the main scheme of substitution:  $\text{Sr}^{2+} + \text{OH}^- \rightarrow \text{Sm}^{3+} + \text{O}^{2-}$  are accompanied by dehydration of hydroxyapatite under the following scheme:  $2\text{OH}^- \rightarrow \square + \text{H}_2\text{O}$ .

#### References

1. T.Kanazawa, Inorganic Phosphate Materials, Elsevier, Amsterdam (1989).
2. S.Sugiyama, K.Abe, T.Minami et al., *Appl. Cat. A:General*, **77**, 169 (1998).
3. S.Sugiyama, T.Minami, T.Higaki et al., *Ind. Eng. Chem. Res.*, **36**, 328 (1997).
4. R.Ramesh, R.J.Jagannathan, *Phys. Chem. B*, **104**, 8351 (2000).
5. J.S.Arey, J.C.Seaman, P.M.Bertsch, *Environ. Sci. Technol.*, **33**, 337 (1999).
6. X.Chen, J.V.Wright, J.V.Conca, L.M.Peurrung, *Environ. Sci. Technol.*, **31**, 624 (1997).
7. R.D.Shannon, *Acta Cryst.*, **A32**, 751 (1976).
8. R.M.Wilson, J.C.Elliott, S.E.P.Dowker, *Amer. Mineralogist*, **84**, 1406 (1999).
9. G.Engel, W.E.Klee, *J. Solid State Chem.*, **5**, 28 (1972).
10. W.E.J.Klee, G.Engel, *J. Inorg. Nucl. Chem.*, **32**, 1837 (1970).
11. A.Serret, M.V.Cabanas, M.Vallet-Regi, *Chem. Mater.*, **12**, 3836 (2000).
12. Taitai, J.L.Lacout, *J. Phys. Chem. Solids*, **7**, 629 (1987).
13. V.O.Hydologkin, V.S.Urusov, K.I.Tobelko, *Geochemistry*, **11**, 1595 (1973).
14. Liao Chun-Jen, Lin Feng-Huci, Chen Ko-Shao, *Biomaterials*, **20**, 1807 (1999).

## Заміщення стронцію на самарій в структурі гідроксиапатиту

**Є.І.Гетьман, О.В.Ігнатов, С.М.Лобода,  
Мухамед А.Б.Абдуль Джабар, А.О.Жегайло, А.С.Глухова**

Методом рентгенофазового аналізу та ІЧ-спектроскопії досліджено ізоморфне заміщення стронцію на самарій в гідроксиапатиті у відповідності до схеми заміщення  $\text{Sr}^{2+} + \text{OH}^- \rightarrow \text{Sm}^{3+} + \text{O}^{2-}$ . Встановлено, що однофазні тверді розчини складу  $\text{Sr}_{10-x}\text{Sm}_x(\text{PO}_4)_6(\text{OH})_{2-x}\text{O}_x$ , синтезовані за температури  $1100^\circ\text{C}$ , утворюються в області  $x = 0-1.6$ . Кристалічну структуру деяких зразків уточнювали за допомогою алгоритму Рітвельда. Встановлено, що іони  $\text{Sm}^{3+}$  переважно локалізуються у позиції Sr(2) структури апатиту. Методом ІЧ-спектроскопії встановлено дегідратацію гідроксиапатиту в отриманих зразках у відповідності до схеми  $2\text{OH}^- \rightarrow \text{O}^{2-} + \square$ .